



Hyperspectral Data Conversion in the Case of Military Surveillance

F. Racek*, T. Baláž and P. Melša

Department of Weapon and Ammunition, University of Defence, Brno, Czech Republic

The manuscript was received on 3 October 2014 and was accepted after revision for publication on 9 June 2015.

Abstract:

The article deals with analysis of raw hyperspectral data conversion. There are mentioned some possible ways of data conversion and their comparison. The comparison is based on both the quality of conversion and the usability in military usage. The analysis is made on the real data taken from the experimental measurement. The quality of conversion is evaluated by matching the converted data with laboratory taken data.

Keywords:

hyperspectral imaging, hyperspectral datacube, spectral reflection, spectral angle mapper

1. Introduction

The science [1] of multispectral (MS) and hyperspectral (HS) imaging is based on taking a part of the electromagnetic spectrum and breaking it into pieces for the purpose of analytical computations. Generally, multiple spectral bands can be used for image formation (see Fig. 1). This way created image is called multivariate or multispectral datacube of dimension $M \times N \times K$. $M \times N$ is a spatial resolution of the datacube and K is the number of spectral bands. Every layer of the datacube represents a narrow band image in certain spectral band λ_i . Another interpretation of the datacube is that it is a set of image vectors, where any image vector is recognized as a spectrum pertained to pixel spatial element. Simply expressed, the whole spectral reflectance of the object in the pixel spatial element is known in the case of HS or MS imaging contrary to the only colour or intensity in the case of traditional imaging.

* Corresponding author: Department of Weapon and Ammunition, University of Defence, Kounicova 65, CZ-662 10 Brno, Czech Republic, phone: +420 973 443 361, E-mail: frantisek.racek@unob.cz

The datacube is called Multispectral up to 100 layers, over 100 layers up to 1000 layers Hyperspectral and over 1000 layers Ultraspectral. If the datacube is formed by the layers with different physical meaning such as narrow band visible image, thermal image and image in polarized light, the datacube is called multivariate and the image vector does not represent spectrum.

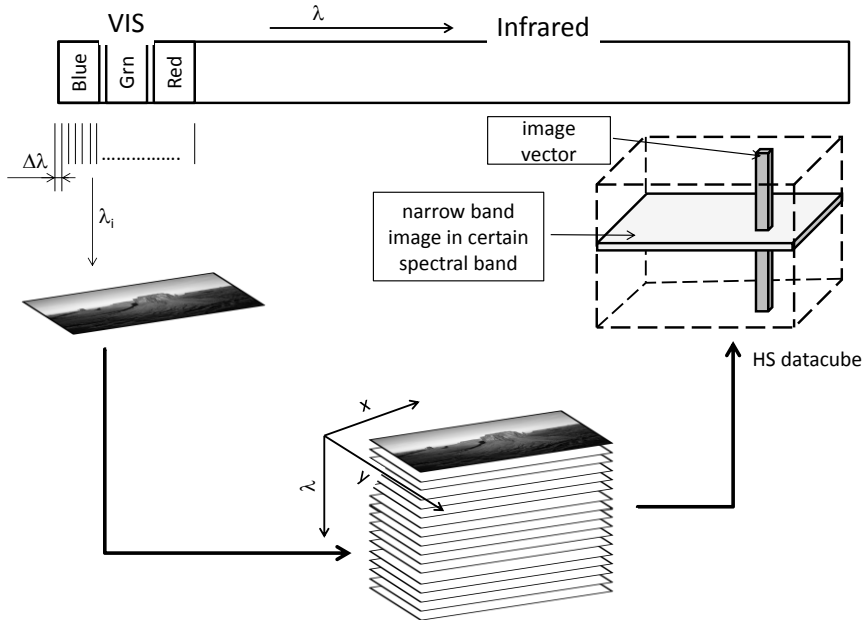


Fig. 1 Creation of HS or MS datacube as a set of layers of narrow band images in narrow spectral bands

Despite the differences between MS and HS datacube, both have significant utilization in military systems. Besides the imaging MS systems focused on specific spectral areas, the MS systems can be utilized for the missile guidance as well as for the protection against them [2]. On the other hand, the Hyperspectral imaging, which is richer in spectral information, is widely used in many areas; for instance in the military it is aimed at hidden or camouflaged target acquisition and surveillance.

2. Methods of Radiance Conversion

Due to the rich spectral information contained in HS datacube, the data processing is aimed at the processing of spectral characteristics of the objects inside the imagined scenery. On the contrary, the spatial pattern recognition techniques common in MS or image processing are assumed as a subsidiary in HS imaging. Thus the HS image processing is focused on the recognition of reflectance spectra of object in the HS image.

Generally, the HS image processing can be divided into two fundamental steps:

- conversion of radiance datacube values into the reflectance values,
- spectra matching.

The spectral target reflectance quality is inherent in datacube, but it is hidden in the signal affected by the conditions under which the measurement was realized.

For the conversion of radiance data into reflectance data, the following methods [3-5] can be used:

- Flat field conversion,
- Average relative reflectance conversion,
- Empirical line conversion,
- Modelling methods.

Average relative reflectance conversion normalizes radiance spectrum dividing it by the value of mean spectra. Mathematically expressed:

$$r(\lambda) = \frac{I(\lambda)}{\bar{I}(\lambda)}, \quad (1)$$

where $r(\lambda)$ is the searched reflectance for spectral band characterized by main spectral wavelength λ , $I(\lambda)$ is the value of recorded radiance for the same spectral band and $\bar{I}(\lambda)$ is the mean value of radiance of all image vectors for the same spectral band characterized by main wavelength λ .

The **flat field conversion** method is based on the assumption that there is an area in the HS image that contains material with flat character of spectral reflectance, so-called flat field. Any image vector is divided by the image vector of flat field to obtain the converted reflectance spectra according to the equation:

$$r(\lambda) = r_{FF} \frac{I(\lambda)}{I_{FF}(\lambda)}, \quad (2)$$

where $I_{FF}(\lambda)$ is the value of radiance image vector of flat field for spectral band characterized by main spectral wavelength λ , r_{FF} is the mean value of the reflectance of the object of the flat field.

Conversion based on the **empirical line conversion** is determined from at least two known objects in the HS image. The object has to be contrastive against the background and has to be large enough to be reliably recognizable. The conversion is then done by:

$$r(\lambda) = \frac{I(\lambda) - I_b(\lambda)}{I_w(\lambda) - I_b(\lambda)} (r_w - r_b) + r_b, \quad (3)$$

where $I_w(\lambda)$ and $I_b(\lambda)$ are the values of radiance of bright object and dark object for the spectral band characterized by the main spectral wavelength λ , respectively. Both dark and bright objects have to feature flat spectral reflectance as well as in the previous case. Reflectance r_w or r_b is the mean values of reflectance of bright or dark object, respectively.

Modelling conversion method is based on the known measurement conditions (sensor quality, season, daytime, atmosphere condition, etc.). The radiance $I(\lambda)$ recorded in image vector can be transformed into the spectral reflectance using the mathematical model $M(\lambda)$ that describes all possible influences. Thus:

$$r(\lambda) = M(\lambda) \cdot I(\lambda). \quad (4)$$

3. Experiment

The methods of data conversion were tested on the data taken from experimental measurements during the year 2013. The data and analyses presented here are illustrated on the HS image (datacube) in Fig. 2. The HS datacube resolution is 1600×1502 pixels and 832 spectral bands. The spectral area is from 398.59 nm up to 1005.16 nm. The scenery in the HS image contains the objects with the typical spectral characteristics to allow both quick visual verification and accurate analysis. The selected objects of interest are sky, cloud, tree #1, bright grass, white, black, bright wall, dark wall, dark grass and tree #2.

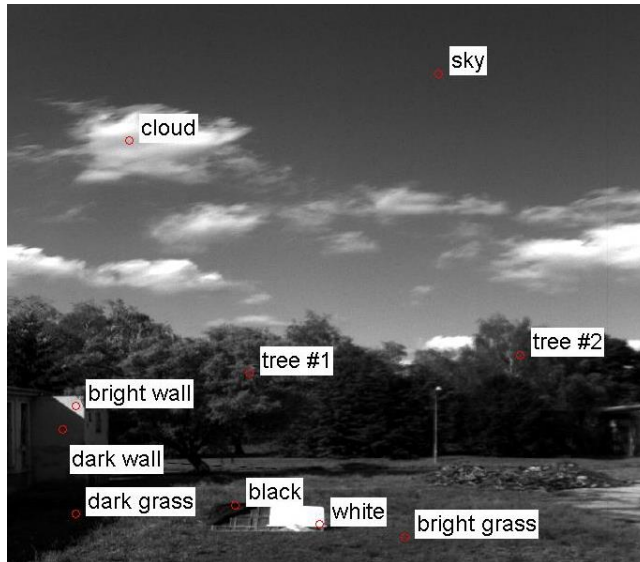


Fig. 2 Test HS image with highlighted objects of interest

Spectral characteristics of the objects of interest are presented in Fig. 3. Radiance spectra of all objects are significantly influenced by spectral characteristics of the light source which was the Sun. The spectral reflectance of the white object (realized by projector screen) is almost constant through the observed spectral region, thus its radiant spectrum very closely matches the solar spectral characteristics on the Earth surface. Despite the fact of solar spectrum effect, the spectral characteristics of vegetation objects (bright grass, dark grass, tree #1, tree #2) feature with the typical signs that are the chlorophyll peak around the wavelength 550 nm and red edge around the wavelength 700 nm.

To simplify the further analysis and data description, the two objects were chosen for the purpose of this article to illustrate the influence of conversion quality on the applied conversion method. The chosen objects are bright and dark grass.

Both; the original raw data of selected objects and converted data are presented in Fig. 4. The result of Average Relative Reflectance Conversion (ARRC) is illustrated in the upper right graph of Fig. 4. The significant advance toward the expected shapes is recognizable. However, the full compensation of solar spectrum was not achieved. Another negative property of this kind of conversion is that it does not guarantee reflectance inside the physically meaningful interval (0, 1).

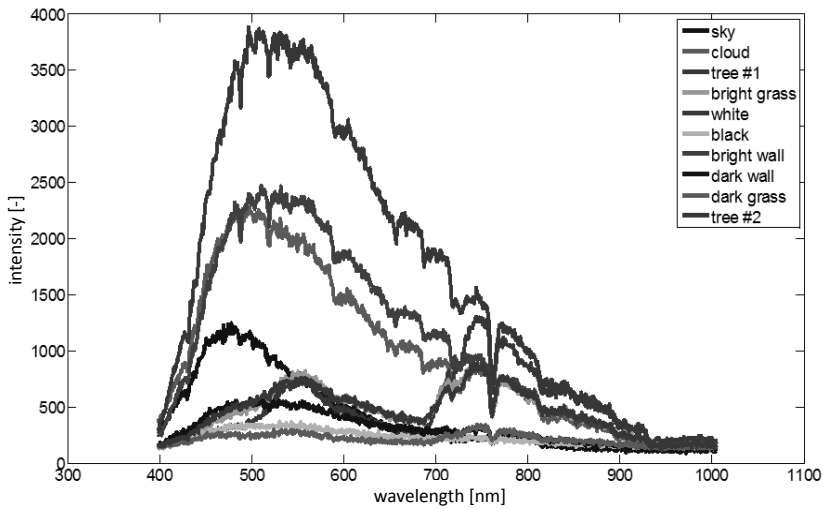


Fig. 3 Spectral characteristics of the objects of interest before conversion

The result of Flat Field Conversion (FFCC) is illustrated in lower left graph of Fig. 4. Again, the converted curves matches quite well the assumed shapes. Both chlorophyll peak and red edge are recognizable. Nonetheless, the spectral curve above red edge should not decrease. Since the white object as the brightest object in the scenery was selected as a flat field (area with the flat spectral curve), the converted curves fall into the physically meaningful interval (0, 1). The spectral curves of dark and bright grass converted due to the Empirical Line Conversion method are illustrated in lower right graph of Fig. 4.

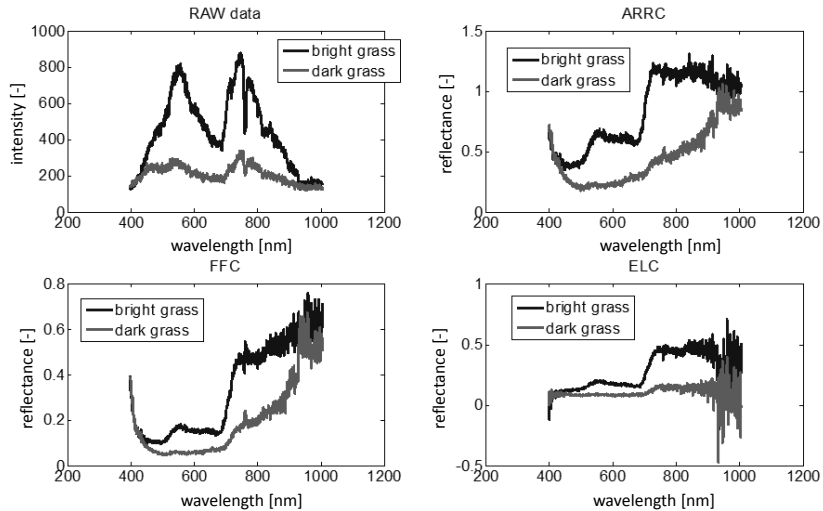


Fig. 4 RAW data and converted spectral reflectance of dark and bright grass objects by different methods

The curves seem to be very well matched with the assumed value and shape. Both chlorophyll peak and red edge are recognizable; the spectral curve is non-increasing above the red edge. However, the dividing by small value (that can also be negative) on the borders of spectral area causes the significant magnification of the noise overlapping the signal. This feature can cause inability to use the converted signal for some methods of subpixel detection or spectral similarity measure.

It is clear from the variety of shapes that the quality of data conversion depends on the method of conversion.

4. Analysis

In the previous chapter, a brief visual evaluation of conversion methods was done. Regular application of HS image requires automatic machine processing. Therefore the conversion quality has to be valorised from that point of view.

Usually, the separated spectral curve from the HS datacube is compared with the spectral curves from the appropriate database in the case of material classification. For this purpose a wide family of similarity measures is used [6, 7]. In our analysis, the procedure will be inverted. The separated spectral curve from the converted datacube is compared with the known spectral curve of appropriate material and the similarity measure is then the indicator of quality of conversion. The Spectral Angle Mapper (SAM) was chosen as the indicator of similarity. SAM was closely described in [8] and it has been proved that it is a robust and reliable tool for matching the spectra. Mathematically, SAM represents the angle between two vectors in N -dimensional space and is expressed:

$$\alpha = \arccos \left(\frac{\sum_{i=1}^N x_i y_i}{\sqrt{\sum_{i=1}^N x_i^2} \sqrt{\sum_{i=1}^N y_i^2}} \right), \quad (6)$$

where x_i and y_i are the elements of compared vectors \mathbf{x} and \mathbf{y} . It is valid for SAM as a similarity indicator that the lower value of SAM represents the higher similarity between signals.

The separated spectra will be compared with the etalon spectra from the database [9]. The spectra of materials which the separated spectrum will be compared with are the spectrum of beech, dry clay, grass, pine tree, sand, stone and wet clay. Of course, the appropriate spectrum is the spectrum of grass. The other spectra are used to test the possibility to correctly distinguish among different spectra. The etalon spectra are presented in Fig. 5.

The result of one step of the analysis is illustrated in Fig. 6. The HS datacube was converted via the ELC method and spectral curves of bright grass were compared with the etalon spectra from the database. It has to be mentioned that not only one image vector (spectral curve) was taken into account, but also 25 image vectors origin from the area of 5×5 pixels. All those 25 curves were compared with etalon spectra, so we have acquired a set of resulting values of SAM. Assuming the set of SAM values as a random variable, we determined the Empirical Probability Density Function (EPDF). The position of the peak m_{SAM} of EPDF was declared as a main value of SAM's random variable. The SAM's main values computed for different etalon spectra have been

compared. As seen in Fig. 6 for assumed case, the grass was found the most similar etalon spectrum with the lowest $m_{SAM} = 0.17$.

We computed the m_{SAM} for all three conversion methods and both chosen objects: bright and dark grass. The results of the analysis are highlighted in Tab. 1. and Tab. 2.

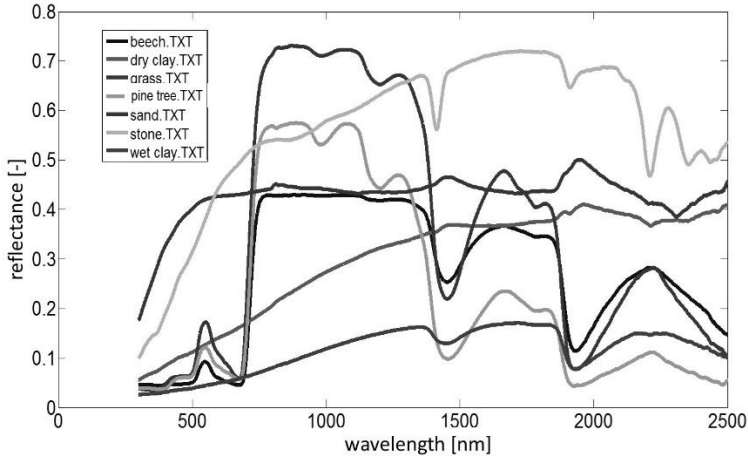


Fig. 5 Etalon spectra

As expected, the results were reached for the object of bright grass. The outcome is caused by higher modulation of image vector and the significant markers like chlorophyll peak and red edge are well recognizable. Contrariwise, due to the low intensity of image vector of dark grass, the significant markers are almost hidden.

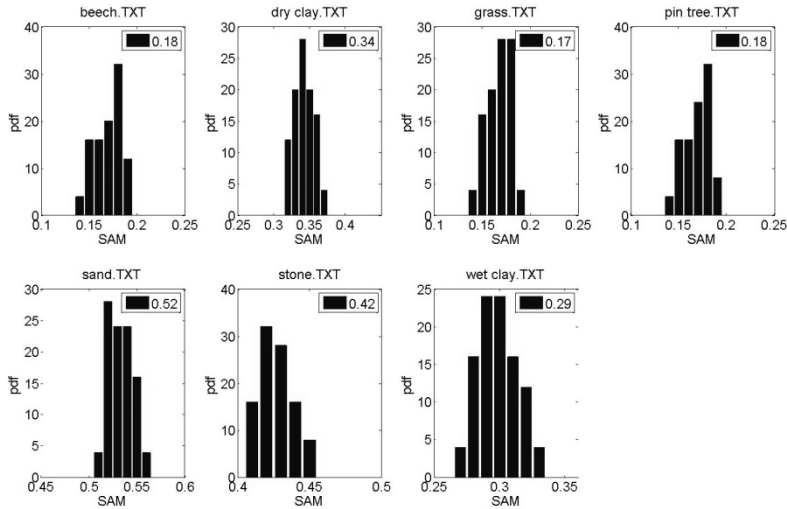


Fig. 6 Analysis result for bright grass and conversion method ELC

Tab. 1 Analysis of similarity of bright grass and etalon spectra

	Beech	Dry clay	Grass	Pine tree	Sand	Stone	Wet clay
ARRC	0.39	0.18	0.31	0.38	0.34	0.23	0.15
FFC	0.18	0.34	0.12	0.18	0.52	0.42	0.29
ELC	0.18	0.34	0.17	0.18	0.52	0.42	0.29

Tab. 2 Analysis of similarity of dark grass and etalon spectra

	Beech	Dry clay	Grass	Pine tree	Sand	Stone	Wet clay
ARRC	0.39	0.18	0.31	0.38	0.34	0.23	0.15
FFC	0.18	0.34	0.12	0.18	0.52	0.42	0.29
ELC	0.18	0.34	0.17	0.18	0.52	0.42	0.29

5. Conclusion

It can be claimed about discussed conversion methods that the best results have been reached for the FFC method. It is valid for both image vectors of dark and bright grass that they were recognized as a vegetation objects. While the image vector of bright grass has been correctly matched with grass etalon, the image vector of dark grass has been recognized as a pine tree. Less evidential results have been reached for ELC method. Only the image vector of bright grass has been successfully recognized as a grass. The image vector of dark grass has not been recognized neither as grass nor as vegetation. Finally, the ARRC method did not guarantee regular conversion on reflectance spectra.

Acknowledgement

The work presented in this paper has been supported by the Ministry of Defence of the Czech Republic (research project PRO K201).

References

- [1] BORENGASSER, H.W.S. and RUSSELL, W. *Hyperspectral Remote Sensing*. Boca Raton: CRC Press, 2007.119 p.
- [2] DOSKOČIL, R. and FARLÍK, R. Self Protections of Aircrafts versus Resistance of Missile Optic Seekers (CM vs. CCM). *Advance in Military Technology*, 2010, vol. 5, no. 2, p. 5-16.
- [3] TNT MIPS, *Introduction to Hyperspectral Imaging* [on line]. Lincoln, Nebraska: MicroImages, 2006. 25 p. [cited 2015-05-06]. Available from: <<http://www.microimages.com/documentation/Tutorials/hyprspec.pdf>>.
- [4] ZHANG, R.J.B. and AZOFEIFA, A.S. Spectral unmixing of normalized reflectance data for deconvolution of lichen and rock mixtures. *Remote Sensing of Environment*, 2005, vol. 95, no. 1, p. 57-66.
- [5] CHANG, C.I. *Hyperspectral Data Exploitation Theory and Application*. Hoboken: Wiley, 2007.

-
- [6] CHEIN, C.I. *Hyperspectral Imaging Techniques for Spectral Detection and Classification*. New York: Cluver Academic/Plenum Publisher, 2003. 370 p.
 - [7] BRUNNER, S. and KARGEL, C. Evaluation of potential emission spectra for the reliable classification of fluorescently coded materials. In *Algorithms and Technologies for Multispectral, Hyperspectral, and Ultraspectral Imagery XVII*, Orlando: SPIE, 2011, p. 80480I-1 – 80480I-15.
 - [8] RACEK, F. and BALÁŽ, T. Analysis of Spectral Angle Mapper as a tool for matching the spectra in Hyperspectral datacube processing. *Advanced in Military Technology*, 2012, vol. 7, no. 2, p. 65-76.
 - [9] BALÁŽ, T. *Optimisation of database of mine optical characteristics ready for hyperspectral imagery* (in Czech) [Research Report]. Brno: VTUO Brno, 2011. 49 p.